Published in final edited form as:
J Comp Neurol. 2010 April 1; 518(7): 1082–1097. doi:10.1002/cne.22265.

Postnatal changes in tryptophan hydroxylase and serotonin transporter immunoreactivity in multiple brain stem nuclei of the rat: implication for a sensitive period

QIULI LIU[1] and **MARGARET T.T. WONG-RILEY**[1]

[1]Department of Cell Biology, Neurobiology and Anatomy, Medical College of Wisconsin, Milwaukee, Wisconsin, 53226, USA

Abstract

Previously, we found that the brain stem neuronal network in normal rats undergoes abrupt neurochemical, metabolic, and physiological changes around postnatal days (P)12–13, a critical period when the animal's response to hypoxia is also the weakest. This has special implications for Sudden Infant Death Syndrome, as seemingly normal infants succumb to SIDS when exposed to respiratory stressors (e.g., hypoxia) during a narrow postnatal window. As abnormal serotonergic system is recently implicated in SIDS, we conducted a large-scale investigation of the 5-HT synthesizing enzyme tryptophan hydroxylase (TPH) and serotonin transporter (SERT) with semi-quantitative immunohistochemistry in multiple brain stem nuclei of normal rats aged P2–21. We found that: 1) TPH and SERT immunoreactivity in neurons of raphé magnus, obscurus, and pallidus, and SERT in the neuropil of the pre-Bötzinger complex, nucleus ambiguus, and retrotrapezoid nucleus were high at P2–11, but decreased markedly at P12 and plateaued thereafter until P21; 2) SERT labeling in neurons of the lateral paragigantocellular nucleus (LPGi) and parapyramidal region (pPy) was high at P2–P9, but fell significantly at P10, followed by a gradual decline until P21; 3) TPH labeling in neurons of the ventrolateral medullary surface was stable except for a significant fall at P12; and 4) TPH and SERT immunoreactivity in a number of other nuclei was relatively stable from P2 to P21. Thus, multiple brain stem nuclei exhibited a significant decline in TPH and SERT immunoreactivity during the critical period, suggesting that such normal development can contribute to a narrow window of vulnerability in postnatal animals.

Keywords

5-HT; critical period; development; raphé nuclei; respiratory control network; serotonin transporter

Introduction

The brain stem neuronal network in rats undergoes abrupt neurochemical, metabolic, and physiological changes during a narrow window of development toward the end of the second postnatal week (around P12–13) (Liu and Wong-Riley, 2002, 2003, 2005; Wong-Riley and Liu, 2005; Liu and Wong-Riley, 2008; Wong-Riley and Liu, 2008). During this critical period, the levels of excitatory neurotransmitters (glutamate) and receptors (NMDA receptors) precipitously fall and those of inhibitory neurotransmitters (GABA) and receptors ($GABA_B$ and glycine receptors) suddenly rise, with a concomitant fall in cytochrome c

Corresponding Author: Margaret T.T. Wong-Riley, Ph.D. Department of Cell Biology, Neurobiology, and Anatomy, Medical College of Wisconsin, 8701 Watertown Plank Road, Milwaukee, WI 53226 Tel.: 1 414 456 8467 Fax: 1 414 456 6517 mwr@mcw.edu.

oxidase activity (a metabolic marker of neuronal activity). The animal's ventilatory and metabolic rate responses to hypoxia are also at their weakest during this time (Liu et al., 2006, 2009). These findings have implications for Sudden Infant Death Syndrome (SIDS), as seemingly normal infants succumb to SIDS when exposed to an external respiratory stressor, such as hypoxia, during a narrow postnatal window of development, peaking at the 2^{nd} to 4^{th} months after birth (Moon et al., 2007).

Recently, abnormality in the serotonergic system has been attributable to the cause of SIDS in human infants (Panigrahy et al., 2000; Narita et al., 2001; Kinney, 2005; Paterson et al., 2006). Serotonin (5-hydroxytryptamine, 5-HT) is involved in the regulation or modulation of numerous functions, including cardiovascular, respiratory, motor, sensory, neuroendocrine, and thermal functions, as well as many behavioral traits, such as arousal, feeding, sexual, cognitive, affective, and aggressive behavior (Zifa and Fillion, 1991; Jacobs and Fornal, 1995; Leysen, 2004). Similar to the noradrenergic and dopaminergic systems, the 5-HT system acts as one of the “level-setting” systems that exert a tonic influence on other systems (Holstege, 2009) and is strongly implicated in the development and patterning of the brain (Lebrand et al., 2006).

In the respiratory system, 5-HT is involved in the modulation of respiratory rhythmogenesis (Bonham, 1995; Hilaire et al., 1997; Hilaire and Duron, 1999; Peña and Ramirez, 2002; Hodges and Richerson, 2008), respiratory motoneuron excitability (Hilaire and Duron, 1999); phrenic long-term facilitation (Fuller et al., 2001; Baker-Herman and Mitchell, 2002), upper airway reflexes (Haxhiu et al., 1998), responses to hypoxic or hypercapnic challenges (Bonham, 1995; Taylor et al., 2005; Penatti et al., 2006; Tryba et al., 2006), and reportedly central chemosensitivity (Richerson, 2004; Richerson et al., 2005; Hodges and Richerson, 2008). 5-HT's action is mediated by various receptor subtypes (mainly 5-HT_{1A}, 5-HT_{1B}, and 5-HT_{2A}), with a net excitatory tonic drive to maintain respiratory output during wakefulness (Richerson, 2004; Hodges and Richerson, 2008). Recently, we found that the immunoreactivity of 5-HT_{2A}R was significantly reduced in several respiratory nuclei during the critical period (around P12) in normal rats (Liu and Wong-Riley, 2008; Wong-Riley and Liu, 2008). Our working hypothesis is that the rate-limiting enzyme of 5-HT biosynthesis, tryptophan hydroxylase (TPH), and the key regulator of 5-HT levels at the synapse, serotonin transporter (SERT), also undergo distinct changes around the critical period. The present study represents a detailed, day-to-day investigation of postnatal development of TPH and SERT in multiple brain stem nuclei of the rat from postnatal day P2 to P21.

Materials and Methods

Tissue preparation

A total of 130 Sprague-Dawley rats, both male and female, from 16 litters were used. All experiments and animal procedures were performed in accordance with the Guide for the Care and Use of Laboratory Animals (National Institutes of Health Publications No. 80–23, revised 1996), and all protocols were approved by the Medical College of Wisconsin Animal Care and Use Committee (approval can be provided upon request). All efforts were made to minimize the number of animals used and their suffering. Rat pups were sacrificed at each of postnatal days P2–P5, P7–P17, and P21 (i.e., 16 time points). At each age, ten (for P10–P14), eight (for P2–5, P7, P17, and P21), or six (for P8, P9, P15, and P16) rats from comparable numbers of ten, eight, or six litters were studied. Rats were deeply anesthetized with 4% chloral hydrate (1 ml/100 g IP; Fisher Scientific, Fair Lawn, NJ) and perfused through the aorta with 4% paraformaldehyde-4% sucrose in 0.1 M sodium phosphate buffered saline (PBS), pH 7.4. Brain stems were then removed and postfixed in the same fixative for 3 h at 4°C. They were subsequently cryoprotected by immersion in increasing

concentrations of sucrose (10, 20, and 30%) in 0.1 M PBS at 4°C, then frozen on dry ice, and stored at −80°C until use.

Antibody characterization

Table 1 summarizes the primary antibodies used in the present study. Both antibodies (anti-SERT and anti-TPH) were well characterized and their specificities established by the manufacturers and previous investigators. The anti-SERT mouse monoclonal antibody (MAB1564, clone 17-7A4, Chemicon, Temecula, CA) was a purified immunoglobulin raised against a rat SERT N-terminus (aa 1–85)/GST fusion protein and its specificity fully characterized by Schroeter et al. (1997). A number of laboratories have used this antibody, notably by Pickel and Chan (1999) at the electron microscopic level, by Brown and Molliver (2000) at the light microscopic level, and by Inazu et al. (2001) with western blotting. The latter group showed two bands (at 73 and 120 kDa) in cortical synaptosomes that correspond to the predicted presence of two possible N-linked glycosylation sites in the extracellular portions of the expressed protein. The anti-TPH mouse monoclonal antibody (T0678, clone WH-3, Sigma, St. Louis, MO) was a purified immunoglobulin raised against a recombinant rabbit TPH and generated from a WH-3 hybridoma. This antibody reacted specifically with tryptophan hydroxylase in immunoblotting assays with a single band of the correct molecular weight of 55 kDa (Sigma). Western blotting of this antibody was also shown by Kish et al. (2008) in human brains. T0678 was also used by a number of investigators, including Burman et al. (2003) and Mulkey et al. (2007) in double-labeling experiments of brain stem serotonergic neurons. In the present study, the labeling of both anti-SERT and anti-TPH antibodies were in the cell bodies of known serotonergic neurons and absent in the cell bodies of non-serotonergic neurons.

Immunohistochemistry

Coronal sections (12-μm thickness) of frozen brain stems were cut with a Leica CM1850 cryostat (Leica Microsystems, Heidelberger, Nussloch, Germany). Seven sets of serial sections were mounted on gelatin-coated slides. In the same litter, sections from 3–4 rats at different ages were mounted on the same slides so that they might be processed together. Ages were grouped typically as follows: P2-10-21, P3-4-5-17, P7-8-9, P11-12-13, and P14-15-16. All sections from all rats were processed under identical conditions (i.e., time, temperature, and concentration of reagents). They were blocked overnight at 4°C with 5% nonfat dry milk-5% normal goat serum-1% Triton X-100 in 0.1 M PBS (pH 7.4). Sections were then incubated at 4°C for 36 h in the primary antibodies diluted at the proper concentration in the same solution as used for blocking: 1:300 anti-SERT or 1:500 anti-TPH. Sections were rinsed 3 times, 5 min each, in PBS, then incubated in the secondary antibodies: 1:100 goat anti-mouse IgG-HRP (Chemicon) for SERT and TPH, diluted in the modified blocking solution (without Triton X-100) for 4 h at room temperature. After rinsing twice with PBS and once with 0.1 M ammonium phosphate buffer (APB), pH 7.0, immunoreactivity was detected with 0.05% DAB-0.004% H_2O_2 in APB for 5 min, and the reaction was stopped with APB for 5 min and then rinsed in PBS three times, dehydrated, and coverslipped. Control sections were processed without primary antibodies or with a non-immune serum in place of the primary antibodies.

For estimates of the percentage of immunoreactive neurons in a specific nucleus, sections from brain stems of an additional litter were processed with Nissl (after TPH-ir or SERT-ir semi-quantitative analysis was finished), which stained all neuronal cell bodies. Another set of alternate sections was reacted for neurokinin-1 receptors, using protocols described previously (Liu and Wong-Riley, 2002).

Brain stem nuclei analyzed

The brain stem nuclei analyzed included the serotonergic neuronal groups (nucleus raphé magnus [RM], nucleus raphé obscurus [ROb], and nucleus raphé pallidus [RP], the ventrolateral medullary surface [VLMS], lateral paragigantocellular nucleus [LPGi], and parapyramidal region [pPy]) and the respiratory related groups (the pre-Bötzinger complex [PBC], nucleus ambiguus [Amb], hypoglossal nucleus [XII], the ventrolateral subnucleus of the solitary tract nucleus [NTS_{VL}], the commissural subnucleus of the solitary tract nucleus [NTS_{COM}], and the retrotrapezoid nucleus [RTN]/parafacial respiratory group [pFRG]). We used a non-respiratory, non-serotonergic nucleus, the cuneate nucleus (CN) as a negative control. CN is known for its relay function in somatosensory transduction but is not involved in respiratory functions.

Semi-quantitative optical densitometry

The immunoreactivity of different markers in the cytoplasm of neurons or in the neuropil in various nuclei studied was semi-quantitatively analyzed by optical densitometric measurements of reaction product of immunohistochemistry, performed with a Zeiss Zonax MPM 03 photometer, a ×25 objective, and a 2-μm-diameter measuring spot. White (tungsten) light was used for illumination, and all lighting conditions were held constant for all of the measurements. Since light intensity can directly affect optical densitometric values, a stepped density filter (Edmund Industrial Optics, Barrington, NJ) with 10-step increments of 0.1 from 0.1 to 1, was used to precisely adjust the intensity of the light source to a standard value identical for all samples.

The boundary of each brain stem nucleus studied was determined with the aid of the Paxinos and Watson's “The Rat Brain Atlas” (Academic Press, New York, 1986), and some of them, including the PBC that was identifiable with the neurokinin-1 receptor labeling (Gray et al., 1999), were described in our previous papers (Liu and Wong-Riley, 2002, 2003, 2005). The RTN was originally described by Smith et al (1989). The pFRG was identified in the neonate with electrophysiological approach, which is located at the rostral ventrolateral medulla, ventrolateral to the facial nucleus and close to the ventral surface (Onimaru and Homma, 2003), and apparently overlaps with the RTN (Feldman and Del Negro, 2006). Since it is not known whether the RTN and pFRG are anatomically and functionally distinct (Feldman and Del Negro, 2006), we referred to this region as `RTN/pFRG'. The part of the nucleus ambiguus chosen for the present study (and our previous studies, Liu and Wong-Riley, 2003, 2005, 2008) was the semicompact formation and the rostral loose formation innervating upper airway muscles and representing pharyngolaryngomotor functions (Bieger and Hopkins, 1987). For the remaining nuclei, measurements were taken from the central main portion of each nucleus.

The optical densitometric value of each labeled neuron in the various brain stem nuclei studied was an average reading of two to four spots in the cytoplasm of its cell body (avoiding the portion that any immunoreactive process crossed the cell body). Only those neurons whose nuclei are clearly visible (i.e., sectioned through the middle of the cell body) were measured. To avoid measuring the same neuron more than once, values were taken from cells in sections at least 70 μm apart, as the largest neurons had a maximal diameter of 25–30 μm, with a maximal nuclear diameter of only about 10 μm. About 100 neurons in each brain stem nucleus were measured for each marker in each rat, and a total of about 1000 (for P10–14), 600 (P8, P9, P15, and P16), or 800 neurons (for the remaining ages examined) for each marker in each nucleus at each age were measured. Comparable numbers of neuropil readings were performed in brain stem nuclei that showed neuropil labeling but not cell body labeling (i.e., 100 readings per brain stem nucleus per rat). For statistical analyses, each sample's optical density value for each nucleus of each rat was the

average of about 100 neurons or neuropil labeling. Thus, the sample number of each time point in each nucleus was ten, eight, or six (representing the number of animals) in Figures 3 and 6. However, the actual number of neurons measured at each time point for each marker was 600, 800, or 1,000. A total of 169,000 neurons and 78,000 neuropil samples were measured for the present study.

Mean optical density values, standard deviations, and standard errors of the mean in each nucleus at each age were then obtained. Statistical comparisons were made among the age groups by using one-way analysis of variance (ANOVA) (to control for the type I comparisonwise error rate) and, when significant differences were found, comparisons were made between successive age groups (e.g., P2 vs. P3, P3 vs. P4, and P5 vs. P7) by using Tukey's Studentized range test (a *post hoc* multiple comparisons, to control for the type I experimentwise error rate). Significance was set at $P < 0.01$ for one-way ANOVA and $P < 0.05$ for Tukey's test.

For photomicrograph production, digital images of immunohistochemically reacted sections were processed with the Photoshop software (Adobe Systems, San Jose, CA) and the contrast and/or brightness of all the images for each nuclear group at different ages were adjusted identically, when and if necessary.

Results

The distribution pattern of TPH and SERT immunoreactivity in neuronal cell bodies and neuropil of various brain stem nuclei analyzed in the present study is outlined in Table 2.

I. TPH-ir neurons in the brain stem nuclei

In general, TPH immunoreactive (-ir) product was clearly observed in the cytoplasm of cell bodies and proximal processes of subpopulations of neurons in the RM, ROb, RP, VLMS, LPGi, pPy, and NTS_{COM}, but were absent or only at background levels in neurons of the other nuclei examined, such as the PBC, Amb, XII, RTN/pFRG, NTS_{VL}, and CN. In general, TPH labeling in the neuropil (other than the proximal dendrites) was relatively low. Control sections without primary antibodies or with non-immune serum showed no specific immunoreactive product above background (data not shown).

The developmental trends of TPH immunoreactivity in the RM, ROb, and RP were similar, but were different from those in the VLMS, LPGi, pPy, and NTS_{COM}. ANOVA revealed significant differences ($P < 0.01$) in TPH immunoreactivity among the ages in the RM, ROb, and VLMS, and Tukey's Studentized range test (comparing one age group with its adjacent younger age group) indicated significant differences (reductions) at P12 for these three nuclei ($P < 0.05$, as compared to the values at P11). P12 was the only time point that yielded statistical significance during the first three postnatal weeks (Fig. 3).

A. TPH immunoreactivity in the RM: TPH-ir was present in ~ 35% – 70% of the RM neurons that were multipolar or pyramid-like in shape and mainly medium in size, which ranged from 10.5 to 14 μm in diameter at P2–P9 to 16 – 18 μm at P11–P21. Immunoreactivity was observed in the cytoplasm and proximal processes, but at a much lower level in the rest of the neuropil (Fig. 1A1–4). Immunoreactivity in the somatic cytoplasm was at a relatively high level from P2 to P11, then it fell significantly at P12 ($P < 0.05$), followed by a plateau at a relatively low level from P13 to P21 (Fig. 3A).

B. TPH immunoreactivity in the ROb: About 70% – 90% of neurons in the ROb exhibited TPH-ir (Fig. 1B1–4). Immunoreactive neurons were mainly small in size and multipolar,

granular, or fusiform in shape. Sizes ranged from 6.5 to 10 μm in diameter at P2–P9 to 7.5 – 12.5 μm at P11–P21. Labeled neuronal processes extended toward the ventral, dorsal, or lateral vicinities, some of them crossing the midline to the contralateral side. The developmental trend of TPH immunoreactivity in ROb neurons was comparable to that of RM (Fig. 3B), with a significant decrease at P12 ($P < 0.05$).

C. TPH immunoreactivity in the RP: Approximately 60% – 80% of neurons in the RP exhibited TPH-ir, and the distribution was similar to those of RM and ROb (Fig. 1C1–4). Labeled neurons were mainly small in size and multipolar, oval, or fusiform in shape. Sizes ranged from 5.5 to 9 μm in diameter at P2–P9 to 6.5 – 12.5 μm at P11–P21. The developmental trend was similar to those of RM and ROb, with a fall at P12 that did not reach statistical significance, followed by a relative plateau until P21 (Fig. 3C).

D. TPH immunoreactivity in the VLMS: On each half of each coronal section through the medulla, there were ~ 1 – 7 TPH-ir neurons distributed along the ventrolateral medullary surface. They were small or medium in size and multipolar or bipolar in shape, with some processes extending mediolaterally or dorsally (Fig. 1D1–4). The size of small neurons ranged from 7 – 10 μm in diameter at P2–P9 to 9 – 12 μm at P11–P21, whereas medium-sized neurons ranged from 10 – 14.5 μm at P2–P9 to 13.5 – 19 μm at P11–P21. The developmental trend of TPH immunoreactivity was relatively constant during the first three postnatal weeks, but with a distinct and significant reduction at P12 ($P < 0.05$) (Fig. 3D). This trend was reminiscent of the one for 5-HT_{2A} receptors in the PBC, Amb, and XII (Liu and Wong-Riley, 2008).

E. TPH immunoreactivity in the LPGi: About 50% – 75% of LPGi neurons were TPH-ir and they were medium or small in size and mainly multipolar or fusiform in shape (Fig. 2A1–4). The size of small neurons ranged from 7 to 11 μm in diameter at P2–P9 to 9 – 13.5 μm at P11–P21, whereas medium-sized neurons ranged from 12 to 15 μm at P2–P9 to 14 – 18 μm at P11–P21. TPH immunoreactivity in LPGi neurons was relatively high during the first postnatal week, decreasing during the second week with a low plateau between P12 and P14, followed by a rise at P15–P16 and a subsequent fall at P17 that was sustained at P21. However, none of these changes reached statistical significance when tested between any two adjacent age groups with the Tukey's test (Fig. 3E).

F. TPH immunoreactivity in the pPy: TPH-ir was observed in about 30% – 65% of neurons in the pPy that were multipolar or fusiform in shape and small or medium in size (Fig. 2B1–4). The size of small neurons ranged from 6.5 to 10.5 μm in diameter at P2–P9 to 9 – 13 μm at P11–P21, whereas medium-sized neurons ranged from 12 to 14.5 μm at P2–P9 to 13.5 – 18.5 μm at P11–P21. TPH immunoreactivity in pPy neurons shared a developmental trend comparable to that in the LPGi, with changes that were not statistically significant (Fig. 3F).

G. TPH immunoreactivity in the NTS_{COM}: TPH immunoreactivity was observed in about 30% – 50% of NTS_{COM} neurons that were small in size and mainly multipolar, granular, or oval in shape (Fig. 2C1–4). Sizes ranged from 5 to 8 μm in diameter at P2–P9 to 8 – 11.5 μm at P11–P21. The developmental trend of TPH immunoreactivity was relatively constant throughout the first three postnatal weeks (Fig. 3G).

II. SERT-immunoreactive (-ir) products in the brain stem nuclei

SERT-ir product was clearly visible in the cytoplasm of cell bodies and proximal processes within subpopulations of RM, ROb, RP, LPGi, pPy, and NTS_{COM} neurons (Fig. 4A–F), but were not visible above background in the cell bodies of PBC, Amb, XII, RTN/pFRG,

NTS_{VL}, and CN neurons (Fig. 5A–F). In the latter six nuclei, labeling was observed in the neuropil surrounding SERT-negative cell bodies, and individual processes were more easily discerned after P11, when neuropil labeling was less intense than those before P11. Control sections without primary antibodies or with non-immune serum demonstrated no specific immunoreactive product above background (data not shown).

There were four developmental trends of SERT immunoreactivity in the various brain stem nuclei examined. The first trend was found in neurons of the ROb and in the neuropil of the PBC and Amb (Figs. 6B, 6G, and 6H), with relatively high levels from P2 to P11, a significant fall at P12 ($P < 0.05$), followed by a plateau at a relatively low level from P13 to P21. The second trend was similar to that of the first, except that the decline at P12 was gradual rather than abrupt, causing it to be statistically not significant. This trend was found in neurons of the RM and RP, and in the neuropil of the RTN/pFRG (Figs. 6A, 6C, and 6I). The third trend was a variation of the first trend, but with a significant reduction at P10 rather than at P12. This was observed in neurons of the LPGi and pPy (Figs. 6D and 6E). The fourth trend was relatively stable throughout the first three postnatal weeks, and it was seen in neurons of the NTS_{COM} and in the neuropil of the XII, NTS_{VL}, and CN (Figs. 6F, 6J, 6K, and 6L). ANOVA indicated significant differences ($P < 0.01$) in SERT immunoreactivity among the ages in the RM, ROb, RP, LPGi, pPy, PBC, Amb, and RTN/pFRG, and Tukey's Studentized range test that compared one age group with its adjacent younger age group indicated significant differences (reductions) at P12 for ROb, PBC, and Amb ($P < 0.05$, as compared to their respective values at P11), and at P10 for LPGi and pPy ($P < 0.05$, as compared to their respective values at P9). P12 and P10 were the only two time points that yielded statistical significance during the first three postnatal weeks for SERT (Fig. 6).

1. SERT labeling in neurons

A. SERT immunoreactivity in the RM: SERT immunoreactivity was present in about 35% – 50% of the RM neurons. They were mainly medium in size and multipolar or pyramid-like in shape. Sizes ranged from 10.5 to 14 μm in diameter at P2–P9 to 16 – 18 μm at P11–P21. Labeling was concentrated in the cell bodies and proximal processes, and was relatively low in the rest of the neuropil (Fig. 4A1–4). The developmental trend of SERT immunoreactivity was an initial dip at P2–P3, a relatively high plateau from P4 to P9, a gradual decline from P9 to P12, and a relatively low plateau until P16, followed by further reductions at P17 and P21 (Fig. 6A).

B. SERT immunoreactivity in the ROb: About 35% – 70% of neurons in the ROb expressed SERT-ir product. These neurons were mainly small in size and multipolar or fusiform in shape, and their labeled processes extended in the ventral, dorsal, or lateral directions, with some crossing to the contralateral side (Fig. 4B1–4). Labeled neurons ranged from 6.5 to 10 μm in diameter at P2–P9 to 7.5 – 12.5 μm at P11–P21. The developmental trend of SERT immunoreactivity was relatively high from P2 to P11, a significant fall at P12 ($P < 0.05$), followed by a plateau of relatively low levels from P13 to P21 (Fig. 6B).

C. SERT immunoreactivity in the RP: SERT immunoreactivity was observed in the cell bodies and some proximal processes of about 50% – 80% of RP neurons (Fig. 4C1–4) that were mainly small in size and multipolar, oval, or fusiform in shape. Sizes of labeled neurons ranged from 5.5 to 9 μm in diameter at P2–P9 to 6.5 – 13.5 μm at P11–P21. The developmental trend of SERT immunoreactivity was a gradual decline from P2 to P11, a more marked but statistically insignificant fall at P12, followed by a relatively low plateau until P21 (Fig. 6C).

D. SERT immunoreactivity in the LPGi: SERT-ir was present in about 20% – 40% of LPGi neurons (Fig. 4D1–4) that were small or medium in size and multipolar and fusiform in shape. Sizes of small neurons ranged from 6.5 – 10.5 μm in diameter at P2–P9 to 8 – 13 μm at P11–P21, whereas medium-sized neurons ranged from 11 to 13.5 μm at P2–P9 to 12.5 – 16 μm at P11–P21. SERT immunoreactivity was relatively high from P2 to P9, a significant fall at P10 ($P < 0.05$), followed by a plateau from P10 to P14, a statistically insignificant rise at P15 and P16, and a further decline at P17 and P21 (Fig. 6D).

E. SERT immunoreactivity in the pPy: About 25% – 50% of neurons in the pPy exhibited SERT-ir, and they were mainly small in size and multipolar, granular, or fusiform in shape (Fig. 4E1–4). Sizes of labeled neurons ranged from 5.5 to 10 μm in diameter at P2–P9 to 6.5 – 12.5 μm at P11–P21. The developmental trend of SERT immunoreactivity was relatively high from P2 to P9, a significant fall at P10 ($P < 0.05$), followed by a plateau at relatively low levels from P11-P16, and a further decline at P21 (Fig. 6E).

F. SERT immunoreactivity in the NTS_{COM}: SERT-ir was present in about 30% – 50% of NTS_{COM} neurons that were mainly multipolar, granular, or oval in shape and small in size (Fig. 4F1–4). Sizes ranged from 5 to 8 μm in diameter at P2–P9 to 8 – 11.5 μm at P11–P21. The developmental trend of SERT immunoreactivity was a gradual but statistically insignificant rise from P2 to P9 followed by a plateau until P17 and a reduction at P21 (Fig. 6F).

2. SERT labeling in the neuropil

A. SERT immunoreactivity in the PBC: SERT immunoreactivity was observed mainly in the neuropil of the PBC, where the level was relatively high from P2 to P11, then a significant fall at P12 ($P < 0.05$), followed by a relatively low plateau until P21 (Figs. 5A1–4, 6G).

B. SERT immunoreactivity in the Amb: The developmental trend of SERT immunoreactivity in the neuropil of Amb was virtually the same as that in the PBC, with relatively high levels from P2 to P11, a significant reduction at P12 ($P < 0.01$), and a plateau of relatively low levels until P21 (Figs. 5B1–4, 6H).

C. SERT immunoreactivity in the RTN/pFRG: SERT labeling in the neuropil of the RTN/pFRG was relatively high during the first postnatal week, followed by a gradual decline until P12, then a relatively low plateau until P21 (Figs. 5C1–4, 6I).

D. SERT immunoreactivity in the XII: SERT immunoreactivity in the hypoglossal nucleus was mainly in the neuropil, with clearly traceable processes distributed within it. Labeling followed a relatively stable trend throughout the first 3 postnatal weeks, with some fluctuations among the ages and attaining the lowest level at P12 (Figs. 5D1–4, 6J).

E. SERT immunoreactivity in the NTS_{VL}: SERT-ir product was present in the neuropil of the NTS_{VL}, where labeled processes traversed across it. The developmental trend was a relative plateau with some fluctuations throughout the first 3 postnatal weeks (Figs. 5E1–4, 6K).

F. SERT immunoreactivity in the CN: SERT immunoreactivity was observed in the neuropil of the CN, where some labeled processes were distributed within it. Labeling was relatively constant throughout the first 3 postnatal weeks (Figs. 5F1–4, 6L).

Discussion

Our comprehensive, in-depth analysis of postnatal TPH and SERT immunoreactivity in multiple brain stem nuclei revealed for the first time that the developmental trends did not follow a straight path during the first three postnatal weeks in rats. Levels were generally high during the first postnatal week, but fell either gradually toward or abruptly at P12, and remained low thereafter until P21. This trend was followed for both TPH and SERT immunoreactivity in neurons of the RM, ROb, and RP, and for SERT in the neuropil of PBC, Amb, and RTN/pFRG. Notably, the fall during the second postnatal week occurred earlier (at P10) for SERT immunoreactivity in neurons of LPGi and pPy. The other general trend was a relatively constant level with some statistically insignificant fluctuations throughout the first three postnatal weeks, and this trend was observed for TPH in neurons of LPGi, pPy, and NTS_{COM}, and for SERT in neurons of NTS_{COM} and neuropil of XII, NTS_{VL}, and CN. A distinct variation of this trend was found in neurons of the VLMS, which exhibited a statistically significant decrease in TPH immunoreactivity only at P12.

Technical limitations

The limitation of immunohistochemistry is that it is dependent on antibody specificity and is not a direct measurement of protein amount. In this regard, western blotting is also reliant on antibody specificity and the amount is generally relative rather than absolute, unless there is a specific protein standard. Whereas immunoblotting can reveal the molecular weight of the immunogen, immunohistochemistry has the distinct advantage of cellular localization within cell bodies and/or neuronal processes in the neuropil. The antibodies used in the current study were monoclonal and well characterized, thus enhancing their specificity. With optical densitometric measurements of immunoreaction product in individual neurons or neuronal processes in the neuropil in clearly identified brain stem nuclei, we were able to extend the analysis to a semi-quantitative level. The large number of neurons/neuropil, the sizeable number of animals, and the close time-course of postnatal ages examined all render credence to the statistical significance obtained in the present study.

Postnatal development of TPH and SERT in various brain stem nuclei

Although 5-HT system is involved in the modulation of numerous functions and behavior, the details of such modulation during postnatal development are poorly understood. To date, relatively little is known about the development of TPH expression in brain stem neuronal network. A relatively high level of TPH immunoreactivity, especially before P12, in neurons of seven brain stem nuclei (current study) is consistent with a high expression of TPH mRNA, protein, and activity postnatally (Park et al., 1986; Rind et al., 2000).

SERT is distributed in the cytoplasm and plasma membrane of cell bodies and axon terminals (Huang and Pickel, 2002) and is, therefore, a more valid marker of serotonergic fibers than 5-HT (Nielsen et al., 2006). SERT mRNA expression reportedly coincides with that of 5-HT immunoreactivity, implying that SERT is primarily expressed in serotonergic neurons (Fujita et al., 1993). However, during development, 5-HT has been postulated to play a “non-traditional” role in neuronal proliferation, migration, and differentiation, as well as in synaptogenesis, neurogenesis, and network organization (Chubakov et al., 1986; Lauder, 1990; Fox, 1992; Ivgy-May et al., 1994; Whitaker-Azmitia et al., 1996; Gould, 1999; Azmitia, 2001; Buznikov et al., 2001; Santarelli et al., 2003; Janusonis et al., 2004; Vitalis et al., 2007; Hodges and Richerson, 2008). In these roles, the expression of SERT, especially in axon terminals, is more widespread during early stage of postnatal development. Our findings of a high level of SERT immunoreactivity during the first 1 ½ postnatal weeks (before P12 or P10) in eight of the twelve brain stem nuclei examined are consistent with an important role for SERT during these early stages of postnatal

development. Even though many of these nuclei do not contain serotonergic neurons, the presence of SERT-immunoreactive fibers prominent especially during the first 1½ postnatal weeks is consistent with serotonin's role in modulating respiratory functions there.

The reduction in SERT immunoreactivity during the second half of the second postnatal week and thereafter in a number of brain stem nuclei may indicate decreased influence of 5-HT as the network begins to mature and increase the activity of its monoamine oxidase A (MAO_A), a catabolic enzyme for 5-HT. Robinson (1968) reported only a weak expression of MAO in the neuropil of the rat brain stem at P5, but by P10 all brain stem nuclei examined have MAO expression varying from weak to intense, and a further increase was found at P15–P20.

Functional implications on the respiratory system

It is well known that multiple brainstem nuclei are involved in respiratory regulation. The PBC is postulated as one of the key centers of respiratory rhythmogenesis (Smith et al., 1991; Rekling and Feldman, 1998; Smith et al., 2000); the Amb and XII control upper airway muscles that are associated with airway patency (Jordan, 2001; Horner, 2007); and the RTN/pFRG glutamatergic neurons have been documented as another major site of central chemoreception (Mulkey et al., 2004; Guyenet et al., 2005, 2008). The NTS_{COM} and NTS_{VL} receive peripheral chemosensitive afferents (Finley and Katz, 1992) and are involved in respiratory modulation (Paton et al., 1991; Bonham, 1995). The medullary raphé (RM, ROb, and RP) serotonergic neurons are involved in cardiovascular regulation (Loewy and Mckellar, 1980) as well as respiratory regulation and presumed central chemosensitivity (Richerson, 2004; Richerson et al., 2005). Likewise, the VLMS serotonergic neurons allegedly contribute to central respiratory chemosensitivity (Richerson et al., 2005). LPGi is one of the most important sources of sympathetic excitatory drive from the medulla to the cardiovascular system (Lovick, 1987). Based on its extensive afferent and efferent connections (Zec and Kinney, 2001; Van Bockstaele et al., 2004), it may integrate respiratory and cardiovascular rhythmic patterns (Gaytán et al., 1997). pPy is reportedly a candidate for central chemoreception (Richerson, 2004; Ribas-Salgueiro et al., 2005). Since LPGi projects to the ventral and dorsal respiratory groups as well as ROb and RP (Smith et al., 1989; Ellenberger and Feldman, 1990; Holtman et al., 1990; Zagon, 1993), and pPy is connected with medullary nuclei subserving cardiorespiratory and other autonomic functions, such as ROb, RP, and the ventral respiratory groups, NTS, and LPGi (Ribas-Salgueiro et al., 2005), and both LPGi and pPy project to the RTN (Cream et al., 2002), it strongly suggests that serotonergic neurons in LPGi and pPy exert a global effect on the other brain stem respiratory nuclei.

The role of 5-HT in modulating respiratory output has long been recognized, but whether its action is excitatory or inhibitory is still under debate, but is likely to be related to the type of receptors that mediate its action (Hilaire and Duron, 1999; Feldman et al., 2003). Transgenic mice lacking 5-HT neurons have severe apnea and a high rate of mortality during postnatal development, indicating that the effect of 5-HT on breathing in vivo is mainly excitatory (Hodges et al., 2009). However, those mice that survived the knockout appeared to markedly improve their respiration between 2 and 4 weeks of age, suggesting that serotonin is more critical during early postnatal weeks than later. This is consistent with our findings that the level of TPH and SERT immunoreactivity is much higher during the first 1½ postnatal weeks (before P12) than later in a number of brain stem nuclei examined.

As a rate-limiting enzyme in 5-HT biosynthesis, TPH expression indirectly reflects serotonergic neurons' functional activity. Inhibition of TPH reportedly reduced the magnitude of the long-lasting respiratory response (Millhorn et al., 1980). SERT is a key protein that limits the systemic availability of 5-HT (Varoqui and Erickson, 1997) and

regulates the entire serotonergic system, including serotonergic receptors via a modulation of serotonin concentration in the extracellular fluid (Horschitz et al., 2001; Pavone et al., 2007). SERT knockout mice exhibited attenuated ventilatory response to hypercapnia (Li and Nattie, 2008).

A major finding of the current study is that TPH and SERT immunoreactivity is significantly reduced in several brain stem nuclei involved in respiratory control (RM, ROb, VLMS, LPGi, pPy, PBC, and Amb) around P12, a critical period of postnatal development when prominent neurochemical, metabolic, and physiological changes occur in the rat's respiratory system (reviewed in Wong-Riley and Liu, 2005, 2008; Liu et al., 2009). Because of serotonin's widespread modulatory effect, a down-regulation of TPH and SERT strongly indicates that respiratory control is compromised around the end of the second postnatal week in normal animals. For some nuclei (RM, ROb, PBC, Amb, and RTN/pFRG), P12 denotes the beginning of a down-regulation of TPH and SERT, suggesting a pruning of the trophic effect of 5-HT. For others, the level of TPH and SERT is maintained throughout the first 3 postnatal weeks. In still others (notably VLMS), the significant fall in TPH immunoreactivity at P12 is returned to the baseline the following day. Interestingly, the down-regulation of SERT in LPGi and pPy neurons preceded the others by two days (i.e., at P10 rather than P12), suggesting that these two nuclei may have a priming effect on the others, especially when they have a widespread brain stem projection (see above). Changes in TPH and SERT may affect other neurotransmitter systems, as the 5-HT system plays a dominant role in the maintenance of well equilibrated neurotransmission (Strüder and Weicker, 2001) via distinct 5-HT receptors, especially 5-HT_{1A} and 5-HT_{1B} presynaptic autoreceptors (Zifa and Fillion, 1992).

The moderate level of SERT sustained in the neuropil of XII, NTS_{VL}, and CN throughout the first 3 postnatal weeks suggests that serotonergic input to these regions is necessary for the neurons' stable functioning. The sustained high immunoreactivity of TPH (and of SERT) throughout the first three postnatal weeks in the NTS_{COM} implies that serotonin is needed by neurons there to perform their normal functions, which include autonomic and respiratory functions as well as carotid chemoreceptor reflexes (Suzuki et al., 2004; Braga et al., 2006).

Clinical implications on SIDS

Previously, we reported that a transient imbalance between excitatory and inhibitory system in respiratory control network occurred during the critical period (Liu and Wong-Riley, 2002, 2005; Wong-Riley and Liu, 2005). A significant reduction in 5-HT_{2A} receptor immunoreactivity was also found at P12 in the PBC, Amb, and XII (Liu and Wong-Riley, 2008). Furthermore, the animal's response to hypoxia is also at its weakest during that time (Liu et al., 2006, 2009). It is intriguing to ask if the rodent's critical period is temporally coincidental with the human's peak incidence of SIDS (2^{nd} to 4^{th} postnatal months), and at least one report indicates that the two time periods are comparable in the two species for brain development (Ballanyi, 2004). SERT binding density in the medulla is reportedly significantly lower in SIDS cases compared to controls (Paterson et al., 2006; Kinney, 2009). It remains to be determined if such a reduction is captured during the normal period of development or if SIDS victims suffer from additional abnormality in the 5-HT system.

Acknowledgments

Supported by NIH grant HD048954 and a grant from the Children's Hospital and Health System Foundation, Milwaukee, Wisconsin. We thank Dr. S. Dhar for helpful discussions.

Literature Cited

Azmitia EC. Modern views on an ancient chemical: serotonin effects on cell proliferation, maturation, and apoptosis. Brain Res Bull. 2001; 56:413–424. [PubMed: 11750787]

Baker-Herman TL, Mitchell GS. Phrenic long-term facilitation requires spinal serotonin receptor activation and protein synthesis. J Neurosci. 2002; 22:6239–6246. [PubMed: 12122082]

Ballanyi K. Neuromodulation of the perinatal respiratory network. Curr Neuropharm. 2004; 2:221–243.

Bieger D, Hopkins DA. Viscerotopic representation of the upper alimentary tract in the medulla oblongata in the rat: the nucleus ambiguus. J Comp Neurol. 1987; 262:546–562. [PubMed: 3667964]

Bonham AC. Neurotransmitters in the CNS control of breathing. Respir Physiol. 1995; 101:219–230. [PubMed: 8606995]

Braga VA, Antunes VR, Machado BH. Autonomic and respiratory responses to microinjection of L-glutamate into the commissural subnucleus of the NTS in the working heart-brainstem preparation of the rat. Brain Res. 2006; 1093:150–160. [PubMed: 16707116]

Brown P, Molliver ME. Dual serotonin (5-HT) projections to the nucleus accumbens core and shell: relation of the 5-HT transporter to amphetamine-induced neurotoxicity. J. Neurosci. 2000; 20:1952–1963. [PubMed: 10684896]

Burman KJ, Ige AO, White JH, Marshall FH, Pangalos MN, Emson PC, Minson JB, Llewellyn-Smith IJ. $GABA_B$ receptor subunits, R1 and R2, in brainstem catecholamine and serotonin neurons. Brain Res. 2003; 970:35–46. [PubMed: 12706246]

Buznikov GA, Lambert HW, Lauder JM. Serotonin and serotonin-like substances as regulators of early embryogenesis and morphogenesis. Cell Tissue Res. 2001; 305:177–186. [PubMed: 11545255]

Chubakov AR, Gromova EA, Konovalov GV, Sarkisova EF, Chumasov EI. The effects of serotonin on the morpho-functional development of rat cerebral neocortex in tissue culture. Brain Res. 1986; 369:285–297. [PubMed: 3697744]

Cream C, Li A, Nattie E. The retrotrapezoid nucleus (RTN): local cytoarchitecture and afferent connections. Respir Physiol Neurobiol. 2002; 130:121–137. [PubMed: 12380003]

Ellenberger HH, Feldman JL. Brainstem connections of the rostral ventral respiratory group of the rat. Brain Res. 1990; 513:35–42. [PubMed: 2350683]

Feldman JL, Del Negro CA. Looking for inspiration: new perspectives on respiratory rhythm. Nat Rev Neurosci. 2006; 7:232–242. [PubMed: 16495944]

Feldman JL, Mitchell GS, Nattie EE. Breathing: rhythmicity, plasticity, chemosensitivity. Annu Rev Neurosci. 2003; 26:239–66. [PubMed: 12598679]

Finley JCW, Katz DM. The central organization of carotid body afferent projection to the brain stem of the rat. Brain Res. 1992; 572:108–116. [PubMed: 1611506]

Fox K. A critical period for experience-dependent synaptic plasticity in rat barrel cortex. J Neurosci. 1992; 12:1826–1838. [PubMed: 1578273]

Fujita M, Shimada S, Maeno H, Nishimura T, Tohyama M. Cellular localization of serotonin transporter mRNA in the rat brain. Neurosci Lett. 1993; 162:59–62. [PubMed: 8121638]

Fuller DD, Zabka AG, Baker TL, Mitchell GS. Phrenic long-term facilitation requires 5-HT receptor activation during but not following episodic hypoxia. J Appl Physiol. 2001; 90:2001–2006. [PubMed: 11299296]

Gaytán SP, Calero F, Núñez-Abades PA, Morillo AM, Pásaro R. Pontomedullary efferent projections of the ventral respiratory neuronal subsets of the rat. Brain Res Bull. 1997; 42:323–334. [PubMed: 9043719]

Gould E. Serotonin and hippocampal neurogenesis. Neuropsychopharmacology. 1999; 21:46S–51S. [PubMed: 10432488]

Gray PA, Rekling JC, Bocchiaro CM, Feldman JL. Modulation of respiratory frequency by peptidergic input to rhythmogenic neurons in the preBötzinger complex. Science. 1999; 286:1566–1568. [PubMed: 10567264]

Guyenet PG, Stornetta RL, Bayliss DA, Mulkey DK. Retrotrapezoid nucleus: a litmus test for the identification of central chemoreceptors. Exp Physiol. 2005; 90:247–253. [PubMed: 15728136]

Guyenet PG, Stornetta RL, Bayliss DA. Retrotrapezoid nucleus and central chemoreception. J Physiol. 2008; 586:2043–2048. [PubMed: 18308822]

Haxhiu MA, Erokwu B, Bhardwaj V, Dreshaj IA. The role of the medullary raphé nuclei in regulation of cholinergic outflow to the airways. J Auton Nerv Syst. 1998; 69:64–71. [PubMed: 9672125]

Hilaire G, Duron B. Maturation of the mammalian respiratory system. Physiol Rev. 1999; 79:325–360. [PubMed: 10221983]

Hilaire G, Bou C, Monteau R. Serotonergic modulation of central respiratory activity in the neonatal mouse: an in vitro study. Eur J Pharmacol. 1997; 329:115–120. [PubMed: 9226402]

Hodges MR, Wehner M, Aungst J, Smith JC, Richerson GB. Transgenic mice lacking serotonin neurons have severe apnea and high mortality during development. J Neurosci. 2009; 29:10341–10349. [PubMed: 19692608]

Hodges MR, Richerson GB. Contributions of 5-HT neurons to respiratory control: neuromodulatory and trophic effects. Respir Physiol Neurobiol. 2008; 164:222–232. [PubMed: 18595785]

Holstege G. The mesopontine rostromedial tegmental nucleus and the emotional motor system: role in basic survival behavior. J Comp Neurol. 2009; 513:559–565. [PubMed: 19235226]

Holtman JR Jr, Marion LJ, Speck DF. Origin of serotonin-containing projections to the ventral respiratory group in the rat. Neurosci. 1990; 37:541–552.

Horner RL. Respiratory motor activity: influence of neuromodulators and implications for sleep disordered breathing. Can J Physiol Pharmacol. 2007; 85:155–165. [PubMed: 17487255]

Horschitz S, Hummerich R, Schloss P. Structure, function and regulation of the 5-hydroxytryptamine (serotonin) transporter. Biochem Soc Trans. 2001; 29:728–732. [PubMed: 11709064]

Huang J, Pickel VM. Serotonin transporters (SERTs) within the rat nucleus of the solitary tract: subcellular distribution and relation to 5HT2A receptors. J Neurocytol. 2002; 31:667–679. [PubMed: 14501206]

Inazu M, Takeda H, Ikoshi H, Sugisawa M, Uchida Y, Matsumiya T. Pharmacological characterization and visualization of the glial serotonin transporter. Neurochem Int. 2001; 39:39–49. [PubMed: 11311448]

Ivgy-May N, Tamir H, Gershon MD. Synaptic properties of serotonergic growth cones in developing rat brain. J Neurosci. 1994; 14:1011–1129. [PubMed: 7509861]

Jacobs, BL.; Fornal, CA. Serotonin and behavior. A general hypothesis. In: Bloom, FE.; Kupfer, DJ., editors. Psychopharmacology: the Fourth Generation of Progress. Raven Press; New York: 1995. p. 461-469.

Janusonis S, Gluncic V, Rakic P. Early serotonergic projections to Cajal-Retzius cells: relevance for cortical development. J Neurosci. 2004; 24:1652–1659. [PubMed: 14973240]

Jordan D. Central nervous pathways and control of the airways. Respir Physiol. 2001; 125:67–81. [PubMed: 11240153]

Kinney HC. Abnormalities of the brainstem serotonergic system in the sudden infant death syndrome: a review. Pediatr Dev Pathol. 2005; 8:507–524. [PubMed: 16222475]

Kinney HC. Brainstem mechanisms underlying the sudden infant death syndrome: evidence from human pathologic studies. Dev Psychobiol. 2009; 51:223–233. [PubMed: 19235901]

Kish SJ, Tong J, Hornykiewicz O, Rajput A, Chang LJ, Guttman M, Furukawa Y. Preferential loss of serotonin markers in caudate versus putamen in Parkinson's disease. Brain. 2008; 131:120–131. [PubMed: 17956909]

Lauder JM. Ontogeny of the serotonergic system in the rat: serotonin as a developmental signal. Ann N Y Acad Sci. 1990; 600:297–313. [PubMed: 2252317]

Lebrand C, Gaspar P, Nicolas D, Hornung JP. Transitory uptake of serotonin in the developing sensory pathways of the common marmoset. J Comp Neurol. 2006; 499:677–689. [PubMed: 17029254]

Leysen JE. 5-HT2 receptors. Curr Drug Targets. 2004; 3:11–26.

Li A, Nattie E. Serotonin transporter knockout mice have a reduced ventilatory response to hypercapnia (predominantly in males) but not to hypoxia. J Physiol. 2008; 586:2321–2329. [PubMed: 18356199]

Liu Q, Wong-Riley MTT. Postnatal expression of neurotransmitters, receptors, and cytochrome oxidase in the rat pre-Bötzinger complex. J Appl Physiol. 2002; 92:923–934. [PubMed: 11842022]

Liu Q, Wong-Riley MTT. Postnatal changes in cytochrome oxidase expressions in brain stem nuclei of rats: implications for sensitive periods. J Appl Physiol. 2003; 95:2285–2291. [PubMed: 12909612]

Liu Q, Wong-Riley MTT. Postnatal developmental expressions of neurotransmitters and receptors in various brain stem nuclei of rats. J Appl Physiol. 2005; 98:1442–1457. [PubMed: 15618314]

Liu Q, Wong-Riley MT. Postnatal changes in the expression of serotonin 2A receptors in various brain stem nuclei of the rat. J Appl Physiol. 2008; 104:1801–1808. [PubMed: 18420721]

Liu Q, Lowry TF, Wong-Riley MT. Postnatal changes in ventilation during normoxia and acute hypoxia in the rat: implication for a sensitive period. J Physiol. 2006; 577:957–970. [PubMed: 17038423]

Liu Q, Fehring C, Lowry TF, Wong-Riley MT. Postnatal development of metabolic rate during normoxia and acute hypoxia in rats: implication for a sensitive period. J Appl Physiol. 2009; 106:1212–1222. [PubMed: 19118157]

Loewy AD, McKellar S. The neuroanatomical basis of central cardiovascular control. Fed Proc. 1980; 39:2495–2503. [PubMed: 6103824]

Lovick, TA. Cardiovascular control from neurons in the ventrolateral medulla. In: Taylor, EW., editor. The neurobiology of the cardiorespiratory system. Manchester University Press; Manchester: 1987. p. 199-208.

Millhorn DE, Eldridge FL, Waldrop TG. Prolonged stimulation of respiration by endogenous central serotonin. Respir Physiol. 1980; 42:171–188. [PubMed: 6452673]

Moon RY, Horne RS, Hauck FR. Sudden infant death syndrome. Lancet. 2007; 370:1578–1587. [PubMed: 17980736]

Mulkey DK, Stornetta RL, Weston MC, Simmons JR, Parker A, Bayliss DA, Guyenet PG. Respiratory control by ventral surface chemoreceptor neurons in rats. Nat Neurosci. 2004; 7:1360–1369. [PubMed: 15558061]

Mulkey DK, Rosin DL, West G, Takakura AC, Moreira TS, Bayliss DA, Guyenet PG. Serotonergic neurons activate chemosensitive retrotrapezoid nucleus neurons by a pH-independent mechanism. J. Neurosci. 2007; 27:14128–14138. [PubMed: 18094252]

Narita N, Narita M, Takashima S, Nakayama M, Nagai T, Okado N. Serotonin transporter gene variation is a risk factor for sudden infant death syndrome in the Japanese population. Pediatrics. 2001; 107:690–692. [PubMed: 11335745]

Nielsen K, Brask D, Knudsen GM, Aznar S. Immunodetection of the serotonin transporter protein is a more valid marker for serotonergic fibers than serotonin. Synapse. 2006; 59:270–276. [PubMed: 16408260]

Onimaru H, Homma I. A novel functional neuron group for respiratory rhythm generation in the ventral medulla. J Neurosci. 2003; 23:1478–1486. [PubMed: 12598636]

Panigrahy A, Filiano J, Sleeper LA, Mandell F, Valdes-Dapena M, Krous HF, Rava LA, Foley E, White WF, Kinney HC. Decreased serotonergic receptor binding in rhombic lip-derived regions of the medulla oblongata in the sudden infant death syndrome. J Neuropathol Exp Neurol. 2000; 59:377–384. [PubMed: 10888367]

Park DH, Snyder DW, Joh TH. Postnatal developmental changes of tryptophan hydroxylase activity in serotonergic cell bodies and terminals of rat brain. Brain Res. 1986; 378:183–185. [PubMed: 3742199]

Paterson DS, Trachtenberg FL, Thompson EG, Belliveau RA, Beggs AH, Darnall R, Chadwick AE, Krous HF, Kinney HC. Multiple serotonergic brainstem abnormalities in sudden infant death syndrome. JAMA. 2006; 296:2124–2132. [PubMed: 17077377]

Paton JF, Rogers WT, Schwaber JS. Tonically rhythmic neurons within a cardiorespiratory region of the nucleus tractus solitarii of the rat. J Neurophysiol. 1991; 66:824–838. [PubMed: 1684382]

Pavone LM, Tafuri S, Mastellone V, Morte RD, Lombardi P, Avallone L, Maharajan V, Staiano N, Scala G. Expression of the serotonin transporter (SERT) in the choroid plexuses from buffalo brain. Anat Rec (Hoboken). 2007; 290:1492–1499. [PubMed: 17957753]

Peña F, Ramirez JM. Endogenous activation of serotonin-2A receptors is required for respiratory rhythm generation in vitro. J Neurosci. 2002; 22:11055–11064. [PubMed: 12486201]

Penatti EM, Berniker AV, Kereshi B, Cafaro C, Kelly ML, Niblock MM, Gao HG, Kinney HC, Li A, Nattie EE. Ventilatory response to hypercapnia and hypoxia after extensive lesion of medullary

serotonergic neurons in newborn conscious piglets. J Appl Physiol. 2006; 101:1177–1188. [PubMed: 16763104]

Pickel VM, Chan J. Ultrastructural localization of the serotonin transporter in limbic and motor compartments of the nucleus accumbens. J Neurosci. 1999; 19:7356–7366. [PubMed: 10460242]

Rekling JC, Feldman JL. Pre-Bötzinger complex and pacemaker neurons: hypothesized site and kernel for respiratory rhythm generation. Annu Rev Physiol. 1998; 60:385–405. [PubMed: 9558470]

Ribas-Salgueiro JL, Gaytán SP, Ribas J, Pásaro R. Characterization of efferent projections of chemosensitive neurons in the caudal parapyramidal area of the rat brain. Brain Res Bull. 2005; 66:235–248. [PubMed: 16023921]

Richerson GB. Serotonergic neurons as carbon dioxide sensors that maintain pH homeostasis. Nat Rev Neurosci. 2004; 5:449–461. [PubMed: 15152195]

Richerson GB, Wang W, Hodges MR, Dohle CI, Diez-Sampedro A. Homing in on the specific phenotype(s) of central respiratory chemoreceptors. Exp Physiol. 2005; 90:259–269. [PubMed: 15728134]

Rind HB, Russo AF, Whittemore SR. Developmental regulation of tryptophan hydroxylase messenger RNA expression and enzyme activity in the raphé and its target fields. Neuroscience. 2000; 101:665–677. [PubMed: 11113315]

Robinson N. Histochemistry of rat brain stem monoamine oxidase during maturation. J Neurochem. 1968; 15:1151–1158. [PubMed: 5711128]

Santarelli L, Saxe M, Gross C, Surget A, Battaglia F, Dulawa S, Weisstaub N, Lee J, Duman R, Arancio O, Belzung C, Hen R. Requirement of hippocampal neurogenesis for the behavioral effects of antidepressants. Science. 2003; 301:805–809. [PubMed: 12907793]

Schroeter S, Levy AI, Blakely RD. Polarized expression of the antidepressant-sensitive serotonin transporter in epinephrine-synthesizing chromaffin cells of the rat adrenal gland. Mol Cell Neurosci. 1997; 9:170–184. [PubMed: 9245500]

Smith JC, Morrison DE, Ellenberger HH, Otto MR, Feldman JL. Brainstem projections to the major respiratory neuron populations in the medulla of the cat. J Comp Neurol. 1989; 281:69–96. [PubMed: 2466879]

Smith JC, Ellenberger HH, Ballanyi K, Richter DW, Feldman JL. Pre-Bötzinger complex: a brain stem region that may generate respiratory rhythm in mammals. Science. 1991; 254:726–729. [PubMed: 1683005]

Smith JC, Butera RJ, Koshiya N, Negro CD, Wilson CG, Johnson SM. Respiratory rhythm generation in neonatal and adult mammals: the hybrid pacemaker-network model. Respir Physiol. 2000; 122:131–147. [PubMed: 10967340]

Strüder HK, Weicker H. Physiology and pathophysiology of the serotonergic system and its implications on mental and physical performance. Part II. Int J Sports Med. 2001; 22:482–497. [PubMed: 11590475]

Suzuki M, Nishina M, Nakamura S, Maruyama K. Benzodiazepine-sensitive GABA(A) receptors in the commissural subnucleus of the NTS are involved in the carotid chemoreceptor reflex in rats. Auton Neurosci. 2004; 110:108–113. [PubMed: 15046734]

Taylor NC, Li A, Nattie EE. Medullary serotonergic neurons modulate the ventilatory response to hypercapnia but not hypoxia in conscious rats. J Physiol. 2005; 566:543–557. [PubMed: 15878953]

Tryba AK, Pena F, Ramirez JM. Gasping activity in vitro: a rhythm dependent on 5-HT2A receptors. J Neurosci. 2006; 26:2623–2634. [PubMed: 16525041]

Van Bockstaele EJ, Pieribone VA, Aston-Jones G. Diverse afferents onverge on the nucleus paragigantocellularis in the rat ventrolateral medulla: Retrograde and anterograde tracing studies. J Comp Neurol. 2004; 290:561–584. [PubMed: 2482306]

Varoqui H, Erickson JD. Vesicular neurotransmitter transporters. Potential sites for the regulation of synaptic function. Mol Neurobiol. 1997; 15:165–191. [PubMed: 9396009]

Vitalis T, Cases O, Passemard S, Callebert J, Parnavelas JG. Embryonic depletion of serotonin affects cortical development. Eur J Neurosci. 2007; 26:331–344. [PubMed: 17650110]

Whitaker-Azmitia PM, Druse M, Walker P, Lauder JM. Serotonin as a developmental signal. Behav Brain Res. 1996; 73:19–29. [PubMed: 8788472]

Wong-Riley MTT, Liu Q. Neurochemical development of brain stem nuclei involved in the control of respiration. Respir Physiol Neurobiol. 2005; 149:83–98. [PubMed: 16203213]

Wong-Riley MT, Liu Q. Neurochemical and physiological correlates of a critical period of respiratory development in the rat. Respir Physiol Neurobiol. 2008; 164:28–37. [PubMed: 18524695]

Zagon A. Innervation of serotonergic medullary raphé neurons from cells of the rostral ventrolateral medulla in rats. Neuroscience. 1993; 55:849–867. [PubMed: 7692351]

Zec N, Kinney HC. Anatomic relationships of the human nucleus paragigantocellularis lateralis: a DiI labeling study. Auton Neurosci. 2001; 89:110–124. [PubMed: 11474639]

Zifa E, Fillion G. 5-Hydroxytryptamine receptors. Pharmacol Rev. 1992; 44:401–458. [PubMed: 1359584]

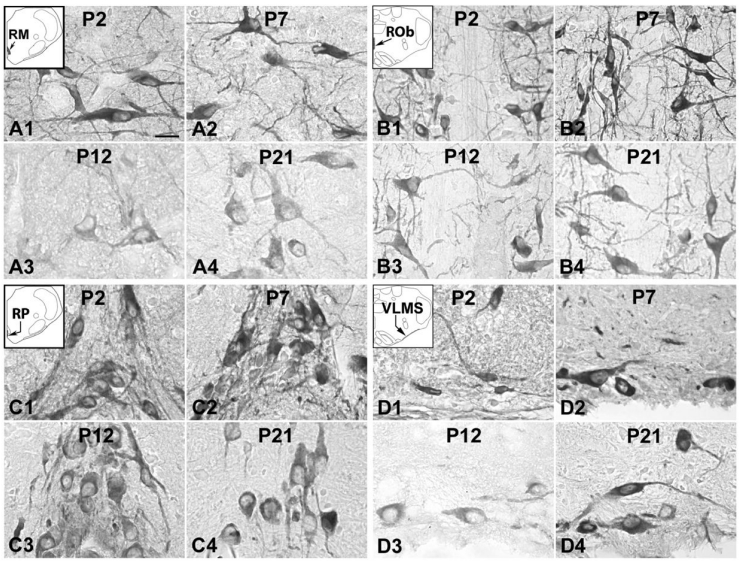

Fig. 1.

Tryptophan hydroxylase (TPH) immunoreactive (-ir) neurons in the nucleus raphé magnus (RM) (A), nucleus raphé obscurus (ROb) (B), nucleus raphé pallidus (RP) (C), and the ventrolateral medullary surface (VLMS) (D) at P2 (A1–D1), P7 (A2–D2), P12 (A3–D3), and P21 (A4–D4). The insets in A1–D1 indicate diagrammatically the locations of these four nuclear groups. TPH expression in the RM, ROb, and RP showed relatively high level at P2 and P7, but relatively low at P12 and P21, whereas that in the VLMS exhibited significantly low level at P12, compared with those in P2, P7, and P21 samples. Scale bar: 20 μm for all.

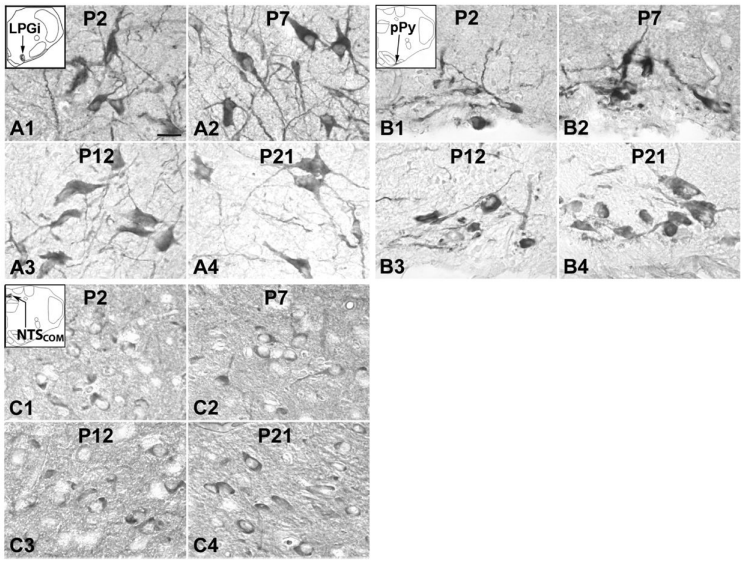

Fig. 2.

TPH-ir neurons in the lateral paragigantocellular nucleus (LPGi) (A), parapyramidal region (pPy) (B), and the commissural subnucleus of the solitary tract nucleus (NTS_{COM}) (C) at P2 (A1–C1), P7 (A2–C2), P12 (A3–C3), and P21 (A4–C4). The insets in A1–C1 indicate diagrammatically the locations of these three nuclear groups. TPH expression in these three nuclei groups exhibited relatively constant level from P2 to P21. Scale bar: 20 μm for all.

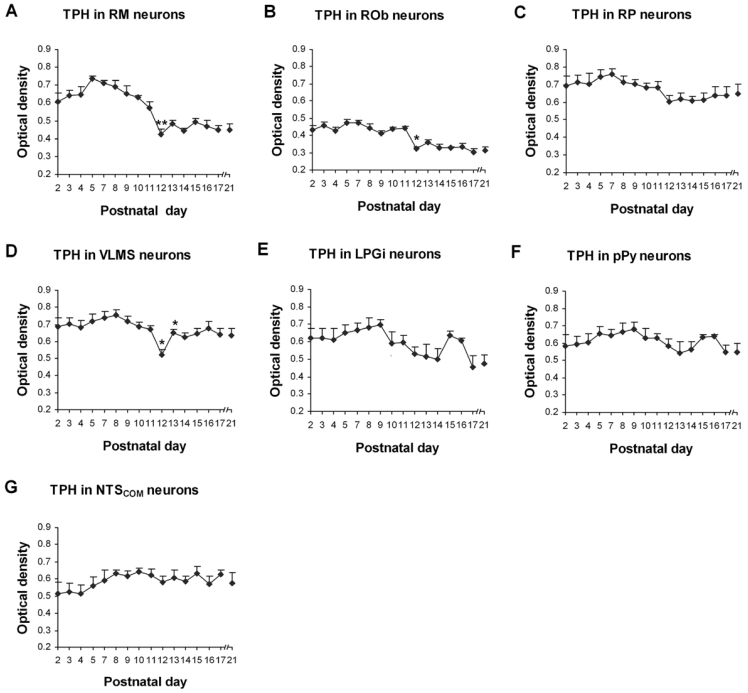

Fig. 3.

Optical densitometric measurements of TPH-ir product in the cytoplasm of individual neurons in the RM (A), ROb (B), RP (C), VLMS (D), LPGi (E), pPy (F) and NTS_{COM} (G) from P2 to P21. Data points were presented as mean ± SEM. Labeling in the first three nuclear groups (A–C) followed a similar trend of development, with initial high levels of expression from P2 to P11, followed by a marked reduction at P12 and remained low thereafter until P21. The developmental pattern in VLMS (D) was relatively stable during the first 3 postnatal weeks, with a distinct and significant fall in TPH expression at P12. On the other hand, the expression in LPGi (E), pPy (F), and NTS_{COM} (G) remained relatively constant from P2 to P21. ANOVA revealed significant differences in TPH expression among ages in the RM, ROb, and VLMS ($P < 0.01$), and Tukey's Studentized test showed a significant reduction in these three nuclei at P12, as compared with their adjacent younger age groups (P11). *, $P < 0.05$; **, $P < 0.01$ (Tukey's Studentized test).

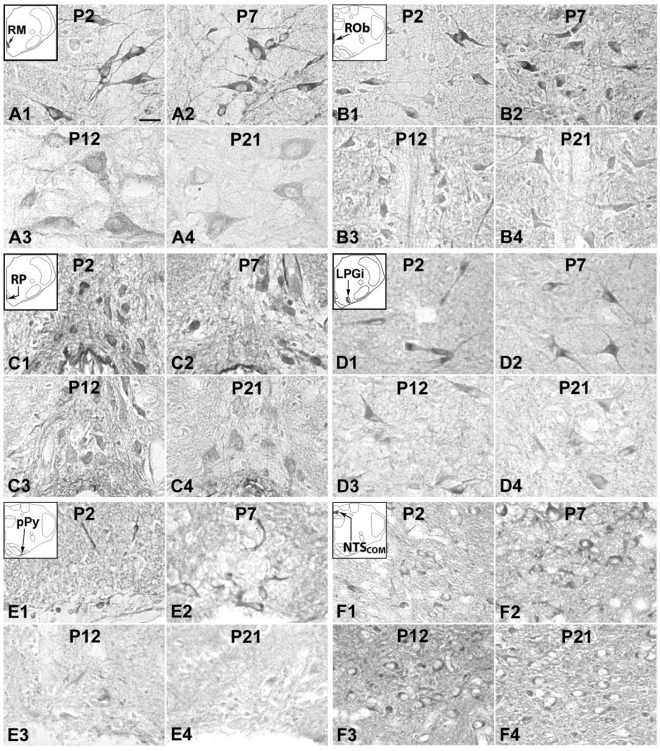

Fig. 4.

Serotonin transporter (SERT) expression in neurons of the RM (A), ROb (B), RP (C), LPGi (D), pPy (E), and NTS_{COM} (F) at P2 (A1–F1), P7 (A2–F2), P12 (A3–F3), and P21 (A4–F4). The insets in A1–F1 indicate the locations of each nucleus in a diagrammatic cross section of the medulla or pons. SERT expression in the RM, ROb, RP, LPGi, and pPy were relatively high at P2 and P7, but were much lower at P12 and P21; On the other hand, the level in NTS_{COM} was quite stable from P2 to P21. Scale bar: 20 μm for all.

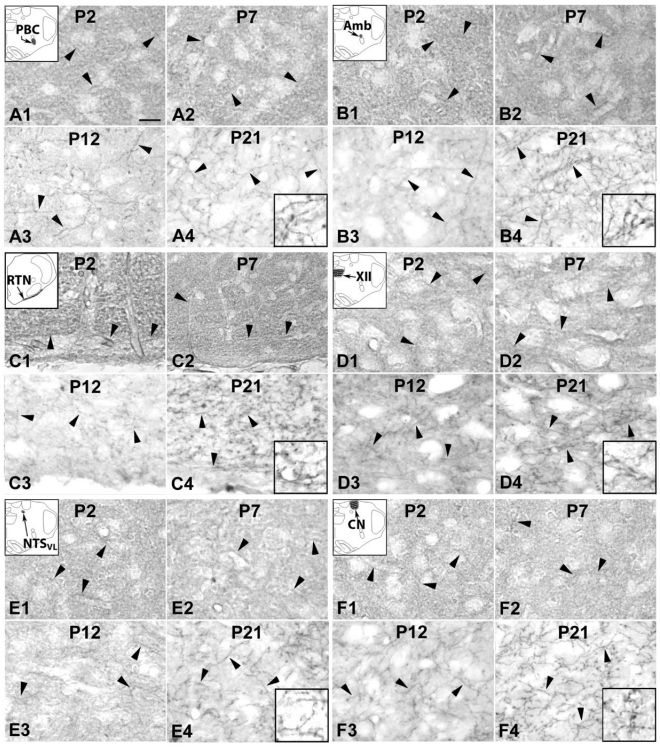

Fig. 5.

SERT expression in the neuropil of the pre-Bötzinger complex (PBC) (A), nucleus ambiguus (Amb) (B), retrotrapezoid nucleus (RTN)/parafacial respiratory group (pFRG) (C), hypoglossal nucleus (XII) (D), ventrolateral subnucleus of the solitary tract nucleus (NTS_{VL}) (E), and cuneate nucleus (CN) (F) at P2 (A1–F1), P7 (A2–F2), P12 (A3–F3), and P21 (A4–F4). The insets in A1–F1 indicate diagrammatically the locations of these six nuclear groups. All arrowheads point to SERT-ir terminal fibers. In these six nuclear groups, the majority of neurons exhibited SERT-negative expression. Scale bar in A1: 20 μm for all except 8 μm for all high magnification insets. See text for details.

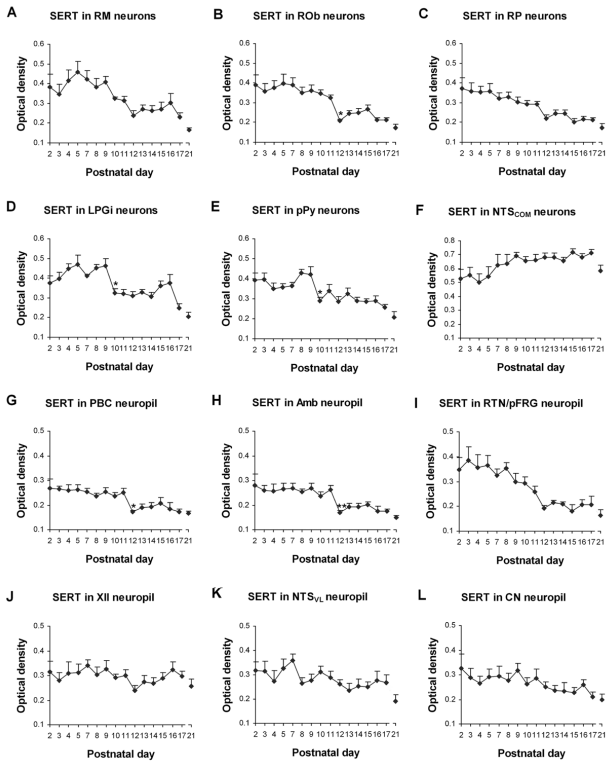

Fig. 6.

Optical densitometric measurements of immunoreactive (-ir) product of SERT in the cytoplasm of individual neurons in the RM (A), ROb (B), RP (C), LPGi (D), pPy (E), and NTS_{COM} (F), as well as in the neuropil of the PBC (G), Amb (H), RTN/pFRG (I), XII (J), NTS_{VL} (K), and CN (L) from P2 to P21. Data points were presented as mean ± SEM. The expressions of SERT in neurons of the RM (A), ROb (B), and RP (C), as well as in the neuropil of the PBC (G), Amb (H), and RTN/pFRG (I) were relatively high during the first 1 to 1 ½ postnatal weeks, then fell significantly or noticeably at P12, followed by a plateau of relatively low levels until P21. In the LPGi (D) and pPy (E) neurons, SERT expression was relatively high at P2–P9, then markedly reduced at P10, followed by a plateau and another decline at P17–P21, except for a small, statistically insignificant peak at P15–P16 in LPGi. On the other hand, labeling in neurons in the NTS_{COM} (F) and in the neuropil of the XII (J), NTS_{VL} (K), and CN (L) was quite stable with only minor fluctuations from P2 to P21. ANOVA yielded significant differences in SERT expressions among the ages in the RM, ROb, RP, LPGi, pPy, PBC, Amb, and RTN/pFRG ($P < 0.01$). Tukey's Studentized test revealed a significant reduction in SERT expression in the ROb, PBC, and Amb at P12, as compared with their adjacent younger age groups (P11), and a significant reduction at P10 in the LPGi and pPy (compared to their adjacent younger age groups P9). *, $P < 0.05$; **, $P < 0.01$ (Tukey's Studentized test).

Table 1

Primary antibodies used.

Antigen	Immunogen	Manufacturer, Species, type, catalog number	Dilution used
Serotonin transporter (SERT)	Rat serotonin transporter, N-terminus (aa 1–85)/GST fusion protein	Chemicon (Temecula, CA), Mouse monoclonal, #MAB1564	1:500
Tryptophan hydroxylase (TPH)	Recombinant rabbit tryptophan hydroxylase	Sigma (St Louis, MO), Mouse monoclonal, #T0678	1:300

Table 2

Distribution of TPH and SERT immunoreactivity in bram stem nuclei of rats

	RM	ROb	RP	PBC	Amb	XII	RTN	VLMS	LPGi	pPy	NTS_{VL}	NTS_{com}	CN
TPH	CB	CB	CB					CB	CB	CB		CB	
SERT	CB	CB	CB	NP	NP	NP	NP	NP	CB	CB	NP	CB	NP

XII, hypoglossal nucleus; Amb, nucleus ambiguus; CB, labeling in neuron cell bodies (and proximal dendrites); CN, cuneate nucleus; LPGi, lateral paragigantocellular nucleus; NP, labeling in the neuropil; NTS_{COM}, the commissural subnucleus of the solitary tract nucleus; NTS_{VL}, the ventrolateral subnucleus of the solitary tract nucleus; PBC, pre-Böotzinger complex; pPy, parapyramidal region; RM, nucleus raphé magnus; ROb, nucleus raphé obscurus; RP, nucleus raphé pallidus; RTN, retrotrapezoid nucleus/parafacial respiratory group; SERT, serotonin transporter; TPH, tryptophan hydroxylase; VLMS, ventrolateral medullary surface.